

Coulomb- and Antiferromagnetic-Induced Fission in Doubly Charged Cubelike Fe-S Clusters

Xin Yang,¹ Xue-Bin Wang,¹ Shuqiang Niu,² Chris J. Pickett,³ Toshiko Ichiye,² and Lai-Sheng Wang^{1,*}¹*Department of Physics, Washington State University, 2710 University Drive, Richland, WA 99352 and W. R. Wiley Environmental Molecular Sciences Laboratory, Pacific Northwest National Laboratory, P.O. Box 999, Richland, Washington 99352*²*School of Molecular Biosciences, Washington State University, Pullman, Washington 99164*³*Department of Biological Chemistry, The John Innes Centre, Norwich Research Park, Colney, Norwich NR4 7UH, United Kingdom*

(Received 31 May 2002; published 26 September 2002)

We report the observation of symmetric fission in doubly charged Fe-S cluster anions, $[\text{Fe}_4\text{S}_4\text{X}_4]^{2-} \rightarrow 2[\text{Fe}_2\text{S}_2\text{X}_2]^-$ ($\text{X} = \text{Cl}, \text{Br}$), owing to both Coulomb repulsion and antiferromagnetic coupling. Photoelectron spectroscopy shows that both the parent and the fission fragments have similar electronic structures and confirms the inverted energy schemes due to the strong spin polarization of the Fe 3d levels. The current observation provides direct confirmation for the unusual spin couplings in the $[\text{Fe}_4\text{S}_4\text{X}_4]^{2-}$ clusters, which contain two valent-delocalized and ferromagnetically coupled Fe_2S_2 subunits.

DOI: 10.1103/PhysRevLett.89.163401

PACS numbers: 36.40.Cg, 36.40.Qv

Fe-S clusters, in particular, the cubelike $[\text{Fe}_4\text{S}_4]$, are ubiquitous in biological systems as active centers in electron transfer proteins [1–5] or as an integral part of the complex catalytic machinery as in hydrogenases and nitrogenases [6–9]. Understanding the structural and electronic properties of the Fe-S clusters and how they are influenced by the protein environments can provide crucial insight into the functionalities of the Fe-S proteins. Synthetic analog complexes have been extremely important to elucidate the structural, electronic, magnetic, and redox properties of Fe-S proteins [1–4]. Various spectroscopic techniques and theoretical methods have been used to investigate the magnetic and electronic structures of the Fe-S clusters in both synthetic analogs and proteins in the condensed phase [1–4, 10–14].

We have developed an experimental technique that combines electrospray ionization (ESI) and photoelectron spectroscopy (PES) to investigate multiply charged anions [15,16]. The ESI technique provides a gentle means to transfer ionic species from solution to the gas phase and is ideally suitable for the study of Fe-S clusters in the gas phase. PES of the gaseous species yields direct information about their electronic structures and intramolecular electrostatic interactions [16]. Figure 1(a) shows the photoelectron spectra obtained for the first time on two doubly charged $[\text{Fe}_4\text{S}_4\text{X}_4]^{2-}$ ($\text{X} = \text{Cl}, \text{Br}$) analog complexes. The $[\text{Fe}_4\text{S}_4\text{X}_4]^{2-}$ dianions were produced using ESI, in ambient conditions, of 10^{-3} M solutions of the respective $[\text{Fe}_4\text{S}_4\text{X}_4]^{2-}$ -containing compounds in pure CH_3CN solvent. Anions produced from the ESI source were transported by a radio-frequency quadrupole ion guide into a 3D quadrupole ion trap, where ions were accumulated for 0.1 s before being pulsed into the extraction zone of a time-of-flight mass spectrometer [15]. The

$[\text{Fe}_4\text{S}_4\text{X}_4]^{2-}$ species were mass selected and decelerated before being intercepted by a probe laser beam in the photodetachment zone of a magnetic-bottle photoelectron spectrometer. Five different detachment photon energies, 532, 355, 266, 193, and 157 nm, were used in the current study (low photon energy data are not shown). The spectral cutoff at the high binding energy side [Fig. 1(a)] is due to the repulsive Coulomb barrier (RCB) that exists universally in multiply charged anions [15–19]. From the photon-energy-dependent PES data, we were able to estimate the RCB, which is a measure of the intracluster Coulomb repulsion for each dianion: 2.1 and 2.0 eV for the Cl and Br complexes, respectively.

Surprisingly, we observed fragmentation products, $[\text{Fe}_2\text{S}_2\text{X}_2]^-$, exactly half of the parents under certain experimental conditions, where collision-induced dissociation (CID) occurs during the ion transport between the ESI source and the ion trap. Figure 1(b) shows the

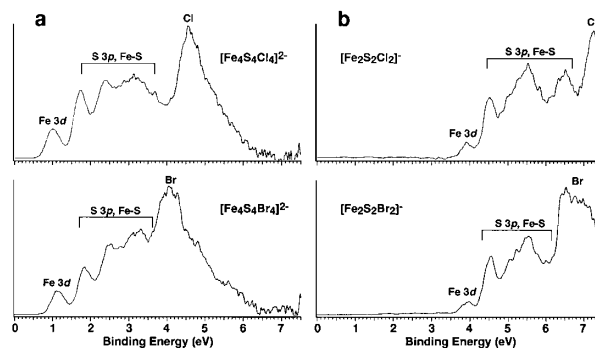


FIG. 1. Photoelectron spectra at 157 nm (7.866 eV) of (a) $[\text{Fe}_4\text{S}_4\text{X}_4]^{2-}$ ($\text{X} = \text{Cl}, \text{Br}$) and (b) their fission daughter ions, $[\text{Fe}_2\text{S}_2\text{X}_2]^-$.

PES data of the two $[\text{Fe}_2\text{S}_2\text{X}_2]^-$ daughter anions, obtained from ESI of $[\text{Fe}_4\text{S}_4\text{X}_4]^{2-}$ samples in a dry nitrogen atmosphere and by operating the instrument with a 2–5 V bias between the ion guide and the ion trap to induce CID [15]. The daughter anions both have much higher electron binding energies because they are now singly charged and lack the intracluster Coulomb repulsion present in the parent dianions. But the spectral features are very similar to the parent in each case, suggesting that the daughter anions and the parent dianions have similar electronic structures as indicated in Fig. 1(b).

Even more remarkably, we confirmed that the $[\text{Fe}_2\text{S}_2\text{X}_2]^-$ species were, in fact, due to a symmetric fission of the parents, $[\text{Fe}_4\text{S}_4\text{X}_4]^{2-} \rightarrow 2[\text{Fe}_2\text{S}_2\text{X}_2]^-$. Mass-selected CID experiments (Fig. 2) show that for $[\text{Fe}_4\text{S}_4\text{Cl}_4]^{2-}$ and $[\text{Fe}_4\text{S}_4\text{Br}_4]^{2-}$ the fission channel is the only fragmentation path. These mass-selected CID experiments were performed on a commercial LCQ (Finnigan, San Jose, CA) electrospray/quadrupole ion-trap mass spectrometer [20]. The anions of interest were first isolated in the ion trap; an ac voltage was then applied to the end caps of the ion trap for ~ 30 ms to drive collisions of the isolated anions with the background gas (10^{-4} Torr N_2). The contents of the ion trap were then analyzed to detect CID products. A single isotopmer could be cleanly isolated and the CID products were identified unambiguously from their isotope distributions.

The symmetric fission in $[\text{Fe}_4\text{S}_4\text{X}_4]^{2-}$ was totally unexpected, because it involves the breaking of four strong Fe-S bonds. Why is it possible among so many other possible fragmentation channels, for example, the loss of one ligand, X? First of all, the intracluster Coulomb repulsion must play a critical role in the fission process, analogous to that in atomic nuclei [21] or multiply ionized metal clusters [22,23]. As mentioned above, the RCB for removing an electron in the two dianions is ~ 2 eV,

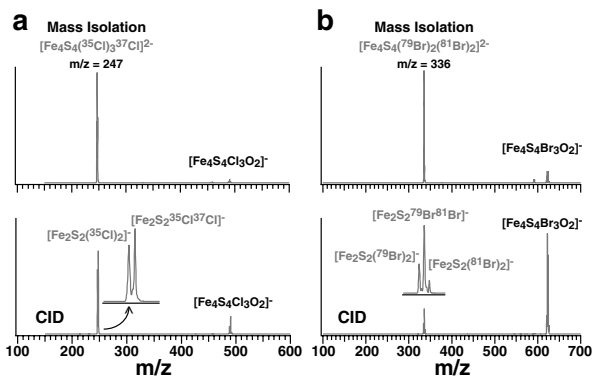


FIG. 2. Collision induced dissociation (CID) of mass-selected anions of (a) $[\text{Fe}_4\text{S}_4\text{Cl}_4]^{2-}$ and (b) $[\text{Fe}_4\text{S}_4\text{Br}_4]^{2-}$. Ligand exchange reaction with residual background O_2 was observed during the CID experiments. All CID fragments are confirmed by their appropriate isotope patterns as shown in (a) and (b).

which is a measure of the magnitude of the intracluster Coulomb repulsion [17] due to the two excess charges in $[\text{Fe}_4\text{S}_4\text{X}_4]^{2-}$. The same amount of Coulomb repulsion is available for the symmetric fission channel. The importance of the Coulomb repulsion for the fission is demonstrated by CID experiments of the singly charged $[\text{Fe}_4\text{S}_4\text{Cl}_4]^-$. This anion has similar structure and bonding as the $[\text{Fe}_4\text{S}_4\text{Cl}_4]^{2-}$ dianion, but its CID is dominated by the loss of Fe and 2Cl; no $[\text{Fe}_2\text{S}_2\text{Cl}_2]^-$ fragment was observed. Nevertheless, the Coulomb repulsion alone is not sufficient to completely account for why the fission channel is preferred over the other possible CID paths in the $[\text{Fe}_4\text{S}_4\text{X}_4]^{2-}$ dianions.

Further insight is provided by the PES data (Fig. 1), which indicate that both the parent and the daughter anions have similar electronic structures. For the $[\text{Fe}_4\text{S}_4]^{2+}$ cubane core, ESR and Mössbauer experiments show that it has no net spins ($S = 0$) and contains two equivalent valent-delocalized $[\text{Fe}_2\text{S}_2]$ sublayers [1–5]. Broken-symmetry density functional theory (DFT) methods have been highly successful in treating the electronic structures of these clusters with weakly coupled high spin centers [12–14]. Figure 3 displays a schematic diagram of the molecular orbital energy levels obtained from the broken-symmetry DFT calculations [14]. As shown in Fig. 3(a), the $[\text{Fe}_4\text{S}_4]^{2+}$ core basically contains two valent-delocalized, ferromagnetically coupled $[\text{Fe}_2\text{S}_2]$ sublayers, which in turn are antiferromagnetically coupled to give the low spin state. There is a large spin polarization of the Fe 3d levels with the majority spin states stabilized by ~ 4 –5 eV. On each $[\text{Fe}_2\text{S}_2]$ sublayer, there are ten majority spins and one minority spin. The $S(3p)$ lone pairs and the Fe-S-based orbitals are spaced in between the majority and minority spin levels

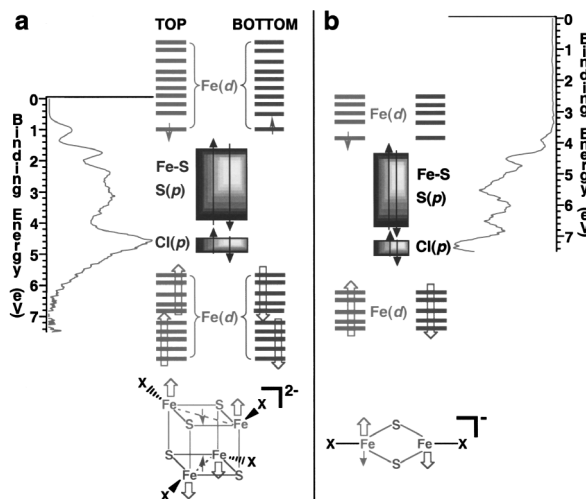


FIG. 3. Schematic inverted energy schemes and comparison with experimental PES data (a) for $[\text{Fe}_4\text{S}_4\text{Cl}_4]^{2-}$ and (b) for $[\text{Fe}_2\text{S}_2\text{Cl}_2]^-$. The thick arrows represent Fe d^5 electron configurations and the small arrows represent a single electron spin.

of the Fe 3*d*, resulting in the so-called inverted level scheme. As labeled in Fig. 1(a) and illustrated in Fig. 3(a), the PES data are in excellent qualitative agreement with this energy scheme, providing yet the most direct confirmation of the validity of the spin couplings and electronic structures of the $[\text{Fe}_4\text{S}_4\text{X}_4]^{2-}$ clusters, as obtained from the broken-symmetry DFT calculations [13,14]. Thus, the $[\text{Fe}_4\text{S}_4\text{X}_4]^{2-}$ clusters can be viewed as two ferromagnets aligned oppositely, but held together by the four strong Fe-S bonds. Upon symmetric fission, the $[\text{Fe}_2\text{S}_2\text{X}_2]^-$ daughter ions again exhibit antiferromagnetic coupling [Fig. 3(b)] [12], giving rise to an inverted energy scheme very similar to the parent dianion. Our PES data of the $[\text{Fe}_2\text{S}_2\text{X}_2]^-$ ions are also in excellent qualitative accord with this energy scheme [Fig. 1(b)]. Hence, the antiferromagnetic coupling not only plays a critical role in the symmetric fission, but also provides the fundamental reason why the parent and daughter anions both exhibit similar electronic structures.

To further confirm the above interpretation, we carried out a preliminary theoretical calculation on the energetics for the symmetric fission of $[\text{Fe}_4\text{S}_4\text{Cl}_4]^{2-}$. The geometry optimizations of the iron-sulfur clusters were performed using the broken-symmetry DFT method with Becke's three-parameter hybrid exchange functional, the B3LYP correlation functional [24], and the 6-31G** basis set [25]. The calculated energies were refined at B3LYP/6-31(++)_SG**//B3LYP/6-31G**, where *sp*-type diffusion functions were added to the 6-31G** basis set of the sulfur atoms [6-31(++)_SG**] [25]. All calculations were performed using the NWChem program package [26].

As shown in Fig. 4, there are two possible symmetric fission channels with either low spin or high spin $[\text{Fe}_2\text{S}_2\text{Cl}_2]^-$ daughter ions. Our calculations suggest that

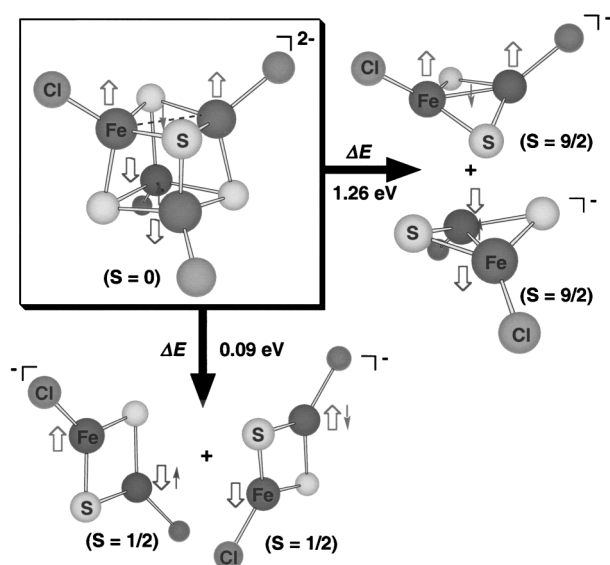


FIG. 4. Calculated energetics for two symmetric fission channels of $[\text{Fe}_4\text{S}_4\text{Cl}_4]^{2-}$.

the low spin products are more favorable by about 1.2 eV, consistent with our PES data [Fig. 3(b)] and previous calculations on $[\text{Fe}_2\text{S}_2]$ model complexes [12–14]. The low spin fission channel is almost thermoneutral with an endothermicity of only 0.09 eV, whereas the high spin fission channel has a much higher endothermicity of 1.26 eV. The average Fe-S bond energy in the $[\text{Fe}_4\text{S}_4]^{2+}$ cubane core was estimated to be ~ 2 eV [27]. Thus, about 8 eV energy would be needed for the symmetric fission, which involves the breaking of four Fe-S bonds. The 2 eV Coulomb energy and the 1.2 eV energy due to the antiferromagnetic coupling account for almost half of the energy required for the symmetric fission. The remaining endothermicity is recovered from the stronger Fe-S bonds in the $[\text{Fe}_2\text{S}_2]$ daughter anions relative to that in the parent [27]. The near thermoneutrality for the symmetric fission of $[\text{Fe}_4\text{S}_4\text{Cl}_4]^{2-}$ to two antiferromagnetic $[\text{Fe}_2\text{S}_2\text{Cl}_2]^-$ is consistent with our observation that the electron loss channel for the two halogen-ligated complexes is not competitive to the fission channel (Fig. 2) because of their relative high electron binding energies (0.76 eV for $[\text{Fe}_4\text{S}_4\text{Cl}_4]^{2-}$, and 0.90 eV for $[\text{Fe}_4\text{S}_4\text{Br}_4]^{2-}$, Fig. 1). Thus, both the intracluster Coulomb repulsion and the antiferromagnetic coupling are important for the observed symmetric fission in the $[\text{Fe}_4\text{S}_4\text{X}_4]^{2-}$ clusters.

Although the symmetric fission in $[\text{Fe}_4\text{S}_4\text{X}_4]^{2-}$ is almost thermoneutral, additional energy acquired during the CID is needed to overcome the fission barrier, analogous to fissions in atomic nuclei or metal clusters [21–23]. However, fission in atomic nuclei or metal clusters is dominated by magic numbers, i.e., certain unusually stable fragments, and symmetric fission is very rarely observed [22,23]. The symmetric fission in $[\text{Fe}_4\text{S}_4\text{X}_4]^{2-}$ is not only due to the intracluster Coulomb repulsion, but also due to the antiferromagnetic coupling in both the parent and daughter anions. The two combined effects lead to the high fissionability of the $[\text{Fe}_4\text{S}_4\text{X}_4]^{2-}$ dianions with no other fragmentation channels observed. The current observation of the symmetric fission and the similarity between the electronic structures of the daughter $[\text{Fe}_2\text{S}_2\text{X}_2]^-$ and the parent $[\text{Fe}_4\text{S}_4\text{X}_4]^{2-}$ proved unequivocally the validity of the broken-symmetry DFT treatment of the Fe-S clusters, providing direct evidence about the spin couplings and the inverted energy schemes within these cubelike clusters [13,14]. Finally, solution phase (redox) interconversion of $\{\text{Fe}_4\text{S}_4\}$ and $\{\text{Fe}_2\text{S}_2\}$ assemblies may well involve related fission or fusion chemistry with reactive $[\text{Fe}_2\text{S}_2\text{X}_2]^-$ intermediates [1–4], now detected for the first time in the gas phase experiments.

We thank Dr. C. Zhou from Professor R. H. Holm's group for providing us the $\text{Fe}_4\text{S}_4\text{X}_4^{2-}$ samples and Dr. S. K. Ibrahim for help with some of the cluster syntheses. CID experiments assisted by Dr. R. J. Moore are gratefully acknowledged. This work was supported by NIH (L. S. W. and T. I.) and BBSRC (C. J. P.). The work was performed at the EMSL, a national scientific user facility

sponsored by the U.S. DOE's Office of Biological and Environmental Research and located at Pacific Northwest National Laboratory, operated for DOE by Battelle.

*To whom correspondence should be addressed.

Email address: ls.wang@pnl.gov

- [1] H. Beinert, R. H. Holm, and E. Munck, *Science* **277**, 653 (1997).
- [2] I. Bertini, S. Ciurli, and C. Luchinat, *Struct. Bonding (Berlin)* **83**, 1 (1995).
- [3] J. A. Ibers and R. H. Holm, *Science* **209**, 223 (1980).
- [4] R. H. Holm and J. A. Ibers, *Iron-Sulfur Proteins III*, edited by W. Lovenberg (Academic, New York, 1977), p. 205.
- [5] H. Beinert, M. C. Kennedy, and C. D. Stout, *Chem. Rev. (Washington, D.C.)* **96**, 2335 (1996).
- [6] J. C. Boyington *et al.*, *Science* **275**, 1305 (1997).
- [7] J. W. Peters, W. N. Lanzilotta, B. J. Lemon, and L. C. Seefeldt, *Science* **282**, 1853 (1998).
- [8] J. Kim and D. C. Rees, *Science* **257**, 1677 (1992).
- [9] B. Schmid *et al.*, *Science* **296**, 352 (2002).
- [10] R. H. Holm, P. Kennepohl, and E. I. Solomon, *Chem. Rev. (Washington, D.C.)* **96**, 2239 (1996).
- [11] *Iron-Sulfur Proteins*, edited by T. G. Spiro (Wiley, New York, 1982).
- [12] L. Noodleman and E. J. Baerends, *J. Am. Chem. Soc.* **106**, 2316 (1984).
- [13] L. Noodleman and D. A. Case, *Adv. Inorg. Chem.* **38**, 423 (1992).
- [14] L. Noodleman, C. Y. Peng, D. A. Case, and J.-M. Mouesca, *Coord. Chem. Rev.* **144**, 199 (1995).
- [15] L. S. Wang, C. F. Ding, X. B. Wang, and S. E. Barlow, *Rev. Sci. Instrum.* **70**, 1957 (1999).
- [16] L. S. Wang and X. B. Wang, *J. Phys. Chem. A* **104**, 1978 (2000).
- [17] L. S. Wang, C. F. Ding, X. B. Wang, and J. B. Nicholas, *Phys. Rev. Lett.* **81**, 2667 (1998).
- [18] M. K. Scheller, R. N. Compton, and L. S. Cederbaum, *Science* **270**, 1160 (1995).
- [19] A. Dreuw and L. S. Cederbaum, *Chem. Rev. (Washington, D.C.)* **102**, 181 (2002).
- [20] D. Zhang and R. G. Cooks, *Int. J. Mass Spectrom.* **195/196**, 667 (2000).
- [21] N. Bohr and J. A. Wheeler, *Phys. Rev.* **56**, 426 (1939).
- [22] U. Naher, S. Bjornholm, S. Frauendorf, F. Garcias, and C. Guet, *Phys. Rep.* **285**, 245 (1997).
- [23] C. Brechignac, Ph. Cahuzac, F. Carlier, and M. de Frutos, *Phys. Rev. Lett.* **64**, 2893 (1990).
- [24] R. G. Parr and W. Yang, *Density-Functional Theory of Atoms and Molecules* (Oxford University Press, Oxford, 1989).
- [25] W. J. Hehre, L. Radom, P. v. R. Schleyer, and J. A. Pople, *Ab Initio Molecular Orbital Theory* (Wiley-Interscience, New York, 1986).
- [26] High Performance Computational Chemistry Group, NWChem, A Computational Chemistry Package for Parallel Computers, Version 4.0.1 (2001), Pacific Northwest National Laboratory, Richland, Washington 99352.
- [27] L. Noodleman, D. A. Case, and E. J. Baerends, in *Density Functional Methods in Chemistry*, edited by J. K. Labonowski and J. W. Andzelm (Springer-Verlag, New York, 1991), pp. 109–123.